α-ZrO_2 DEPOSITION INSIDE HOLLOW SUBSTRATES BY REMOTE PLASMA ENHANCED CHEMICAL VAPOR DEPOSITION. MODELING OF THE PROCESS.

T. Belmonte, V. Guérold, H. Michel

Laboratoire de Science et Génie des Surfaces (UMR 7570),
Ecole des Mines de Nancy, Institut National Polytechnique de Lorraine, Parc de Saurupt,
54042 Nancy cedex, France.

Corresponding author : T. Belmonte. fax number : 03-83-57-42-35. e-mail : belmonte@mines.u-nancy.fr

ABSTRACT

Deposition inside hollow substrates of zirconia in late Ar-O_2-H_2 post-discharges Is considered. Inner surface of cylindrical substrates of about two tens centimeters long could be coated by this process over their whole length with a thin film of zirconia from 573 K upwards.
A complete modeling was required to control the process. Resolution of the conservation equations of continuity, momentum and energy was carried out. Indeed, by this mean, the thickness homogeneity of layers were improved to lead to almost constant or weakly decreasing deposition rates along the substrate.

1. INTRODUCTION

ZrO_2 has low electric conductivity and extreme chemical inertness. ZrO_2 is suitable for applications in semi-conductor devices[1], thermal barrier coatings[2], or oxidation resistance coatings[3]. Its deposition inside hollow substrates could be an interesting solution to the problem of wear that occurs, for example, in extrusion dies.
In a recent paper[4], RPECVD of zirconia in late Ar-O_2-H_2 post-discharges was considered (species reach the substrate after about 25 ms). Outer surface of cylindrical substrates of about two tens centimeters long could be coated by this process over their whole length with a thin film of zirconia from 573 K upwards.
Plasma assistance was first chosen because oxidation of $ZrCl_4$ by O_2 was impossible at low temperatures that are needed on metallic alloys which are treated thermally or thermochemically and whose structures can be damaged by high temperatures. Reaction between $ZrCl_4$ and water was assumed to be very difficult as stated in the literature[5].
Indeed, before our work, no result was available on $ZrCl_4$ hydrolysis between 573 K and 753 K for this reason that handling water was described to lead to unsuitable results[5].
As the highest deposition rates were obtained in our RPECVD process for a plasma composition of Ar-12.5vol.%O_2-24vol.%H_2, i.e. the stoichiometry for water synthesis, a complete characterization of the late post-discharge was carried out. Water presence was observed in the late post-discharge with no doubts. A comparison was drawn between the RPECVD process and the hydrolysis of $ZrCl_4$ by conventional CVD. In the temperature range [573 K-753 K], the reaction pathway for zirconia deposition was demonstrated to be the hydrolysis of the zirconium tetrachloride. The use of a plasma in this case was a very simple mean to determine a partial pressure of water at the inlet of the reaction zone. It was concluded that our RPECVD process was, in the late post-discharge and in the range of temperature given above, comparable with a conventional hydrolysis process.
It could be pointed out that the hydrodynamic conditions leading to zirconia formation are very precise. Consumption of the reactive species in the gas phase is low enough to ensure a powder size that remains low while they flow in the reactor to be evacuated. But partial pressures of reactive species remains high enough to get a significant deposition rate on the substrate ($\approx$10 $\mu m\ h^{-1}$). These conditions depend on the kinetics of $ZrCl_4$ hydrolysis which is mainly controlled by the temperature , which the effect on reaction kinetics was determined, and by the partial pressures of water and zirconium tetrachloride. The partial pressures of the reactive species have to be low enough between 573 K and 753 K to ensure a reproducible deposition process. For this reason, modeling is required to control the process. Indeed, by this mean, the thickness homogeneity of layers can be improved to lead to almost constant or weakly decreasing deposition rates along the substrate. Many works on CVD modeling were carried out with this aim[6-22].
In this paper, conclusions of our previous study are extended to the case of hollow substrates. A short study of the influence of various parameters is carried out and correlated to a modeling of the reactor.

2. EXPERIMENTAL APPARATUS

The RPECVD apparatus consists of three parts : 1) the microwave excitation of an Ar-O_2-H_2 mixture (SWL); 2) a chlorination chamber to perform $ZrCl_4$ in-situ synthesis (CL) and 3) the furnace where the substrate is located (S) (figure 1). The transport of the excited species to the substrate is ensured by a tube which also separates them from other gases.

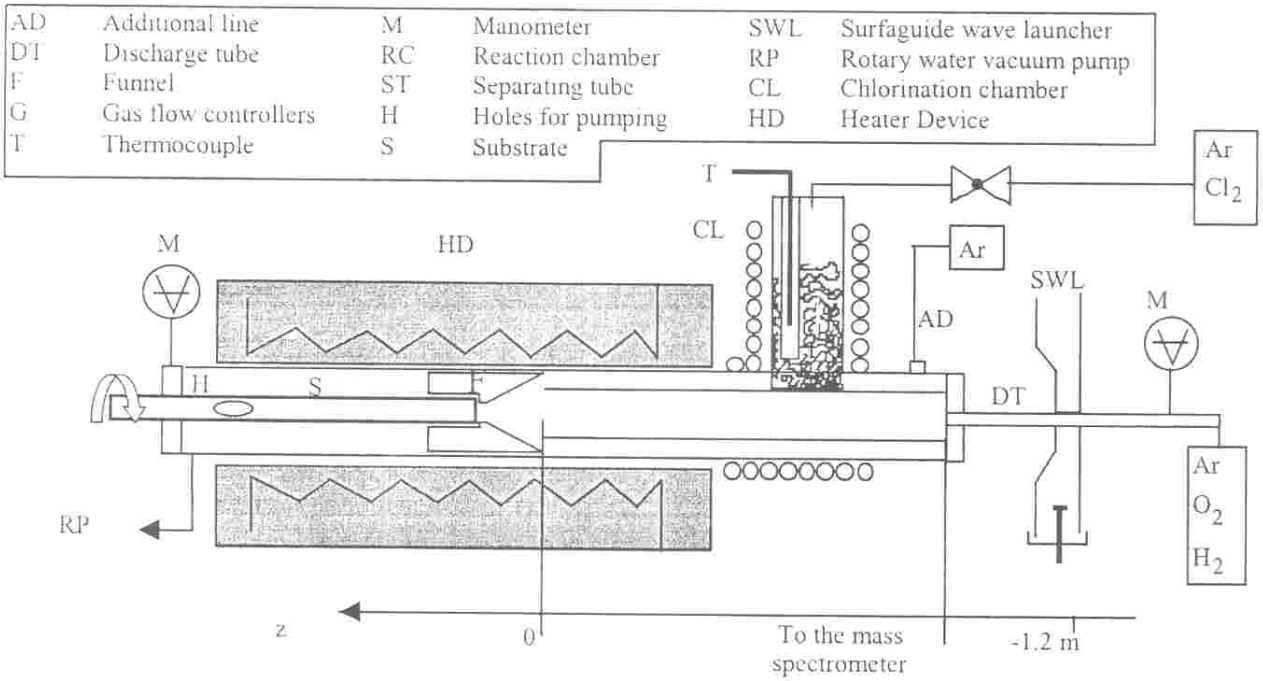

Figure 1 : Experimental device

The plasma source is produced in a quartz tube (5 mm inner diameter) by a 2.45 GHz microwave system with a surfaguide surface wave launcher located upstream (1.2 m) from the deposition chamber. Delivered power is constant (130 W).

To avoid gas phase reactions, the oxidizing mixture flows through the discharge and reaches the reaction zone in a quartz tube (15 mm inner diameter) separating this oxidizing mixtures from the Ar-$ZrCl_4$ mixture. Typical gas flow rates are indicated in table 1. Each species except argon can then be considered as very diluted.

The chlorination chamber is an in-situ synthesis device of $ZrCl_4$ from an Ar-Cl_2 mixture flowing through a zirconium bed heated to 623 K (except when the furnace temperature is lower. In this case, the chlorination temperature is equal to the furnace one). The reaction $Zr + 2Cl_2 \rightarrow ZrCl_4$ is complete under conditions of temperature and pressure, what is verified by mass loss measurements. Argon flow rate in the chlorination chamber is 21 sccm while Cl_2 is in the [0 - 5 sccm] range. As this flow rate is low, compared to that of the post-discharge, an additional argon line enables to increase the total flow rate of $ZrCl_4$ without changing the chlorination yield. Argon flow rate in this additional line is 600 sccm.

The reactor is a quartz tube (inner diameter of 28 mm). The substrate is located 1.20 m downstream from the gap discharge, in a furnace with an isothermal zone of 30 cm. Temperature is varied between 573 K and 753 K.

The substrate is a cylinder (9.5 mm outer diameter) of 20 cm length. A holder, with the same cylinder shape, penetrates the end of the substrate and supports it. It rotates to ensure a constant radial deposition rate distribution. Rotation is considered low enough (actually 0.6 rad s^{-1}) to ignore any possible pressure diffusion effect. Therefore, $ZrCl_4$ distribution is assumed to be cylindrical. The end of the substrate has holes for pumping.

Table 1 : Reference conditions

General conditions
T = 753 K
P = 15 hPa
Discharge parameters
Pw = 130 W
Q_{Ar} = 1027 sccm
Q_{O2} = 12.5 sccm
Q_{H2} = 24.5 sccm
H_2O partial pressure at z=0 : 22.5 Pa
Chlorination conditions
T = 623 K
Q_{Ar} = 21 sccm
Q_{Cl2} = 5 sccm
Additional line : 600 sccm

Mixture of the gases and their introduction in the substrate are done by the way of a ceramic funnel. The cone of the funnel is 45 mm long and 9 mm high between its inner and outer walls.

3. MATERIAL RESULTS

Experiments are carried out between 573 K and 753 K in the conditions specified in Table 1. The deposition rates are calculated from SEM micrographs. The substrate, after treatment, is sawed in pieces of one centimeter long, and submitted to a mechanical strain till the layer broke. These

results will be compared hereafter with calculated deposition rates.

For a given temperature, the same morphology was obtained all along the substrate. As described in reference[23], at 573 and 673 K, divergent polycrystalline sheaths are formed, each composed of several columnar single crystals. At 753 K, the "columns" are composed of individual straight-sided single crystals. But the average diameter of each crystal varies with temperature. It can be concluded that density of the layer increases when temperature increases.

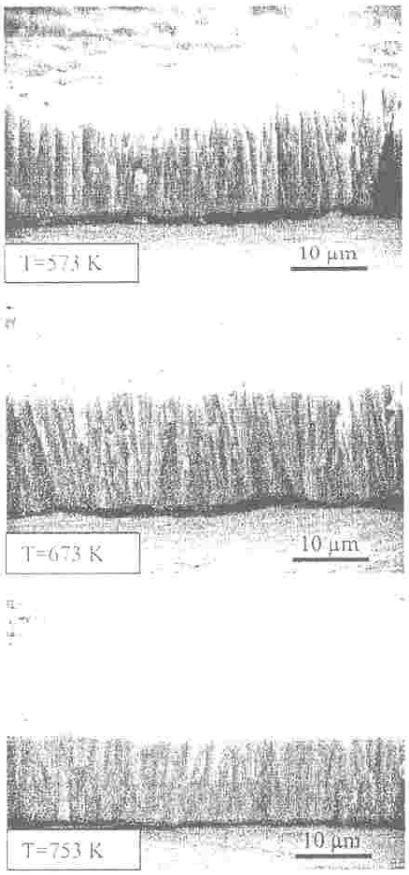

Figure 2 : SEM micrographs of cross sections of substrates treated at (a) 573 K, (b) 623 K, (c) 753 K in conditions of table 1.

The presence of particles in the layer is to be expected at higher temperatures[24] but is barely observed between 573 and 753 K. Furthermore, the reaction rate in the gas phase do not lead to a complete consumption of reactants and deposition occurs at significant rates.

4. MODELING

4.1 HYDRODYNAMIC MODELING

The model used in this study is obtained by solving the conservation equations of continuity, momentum and energy. Equations are solved considering a stationary state. Pressure in the system is large enough to consider the gas phase as satisfying the equations in a continuum medium (Kn =2 10^{-3}). The set of partial differential equations which expresses the conservation of component i (what leads to the continuity equation by summing over i), the momentum and energy balance is closed by the ideal gas law :

$$(1) \qquad \nabla.(\rho\omega_i\vec{v} - D_i\rho\vec{\nabla}\omega_i) = S_{\omega i}$$

$$(2) \qquad \nabla.\rho\vec{v}\vec{v} - \nabla.\bar{\bar{\tau}} = -\vec{\nabla}P + \rho\vec{g}$$

$$(3) \qquad \nabla.(\rho C_p T\vec{v} - k\vec{\nabla}T) = 0$$

ρ is the fluid density; $\vec{v}$ the velocity; ω_i the mass fraction and $S_{\omega i}$ is the consumption source of the reactive species (the deposition kinetics) as specified further. The species balance (1) can be solved to yield the mass fraction fields. Each reactive species is assumed to be dilute in argon, allowing for the use of a simple form of Fick's law. D_i is then considered as the binary diffusion coefficient in argon.

$\bar{\bar{\tau}}$ is the stress tensor. $\rho\vec{g}$, T, P, Cp and k are respectively the gravitation force, fluid temperature, pressure, specific heat at constant pressure and thermal conductivity. The flow is assumed to be laminar (Re<150). Convection regime is forced ($Gr/Re^2<10^{-5}$). Soret diffusion is herein ignored. All the transport data are given in table 2.

Table 2 : Transport data

$\lambda_{Ar} = 3.71\ 10^{-5}\ T + 7.31\ 10^{-3}$ W m^{-1} K^{-1}
$\mu_{Ar} = 3.81\ 10^{-8}\ T + 1.57\ 10^{-5}$ kg m^{-1} s^{-1}
$Cp_{Ar} = 520$ J kg^{-1} K^{-1}
$D_{ZrCl4\text{-}Ar} = 6\ 10^{-5}\ T^{1.75}/P$ m^2 s^{-1}
$D_{H2O\text{-}Ar} = 3\ 10^{-4}\ T^{1.5}/P$ m^2 s^{-1}

A dilute medium is the key parameter to the simplicity of our model. It is also, as we are going to see it later, the reason of the excellent control of the process.

4.2 KINETICS MODEL

In a previous paper[4], a study of the possible reaction pathways leading to the deposition of the ZrO_2 films establishes that, in the range [573 K-753 K], the main reaction leading to zirconia formation is :

(a) $ZrCl_4+2H_2O \rightarrow ZrO_2+4HCl$

This reaction pathway was applied to the heterogeneous reaction. It is also applied to gas phase reaction but with a different rate constant. This is necessary to take into account the reactant depletion due to the gas phase consumption. It is observed that in the RPECVD process, hardly no particle formed in the gas phase falls onto the film. It is known[5] that at high temperature (1223 K), unsuitable results are obtained when water reacts with a chloride. This is due to the violent reaction between these two species which leads to particle formation and reactant consumption. Between 573 K and 753 K, particle size is probably smaller because the reaction rate is less fast and because the particles do not agglomerate while they stay in

the furnace. These small size particles are then carried away by the gas flow. The depletion due to the consumption of the reactive species in gas phase is weak enough to ensure a deposition rate of a few micrometer per hour. Nevertheless, this depletion is not negligible. Indeed, this phenomenon explains how the deposition rate on the substrate can remain constant with a temperature change of about a hundred degrees as it will be presented hereafter.
Therefore, two simple coupled chemical reactions are assumed for consumption of gaseous precursors.
Gas phase and surface reactions can be written as follows :

$$ZrCl_4 + 2H_2O \xrightarrow{k_{s,v}} ZrO_2 + 4HCl \quad (4)$$

where $k_{s,v}$ is the rate constant for surface or gas phase reaction. The source terms of equations of continuity for A and B are therefore due to the gas phase consumption:

$$S_{\omega ZrCl4} = -k_v \rho \omega_{ZrCl4} \left(\frac{\rho \omega_{H2O}}{M_{H2O}}\right)^2$$

$$S_{\omega H2O} = -2k_v \frac{\rho \omega_{ZrCl4}}{M_{ZrCl4}} \frac{(\rho \omega_{H2O})^2}{M_{H2O}} \quad (5)$$

The growth rate is then defined by :

$$v_d = \frac{M_{ZrO2}}{\rho_{ZrO2}} \vec{J}_{ZrCl4}.\vec{n} \quad (6)$$

where $\vec{J}_{ZrCl4}$ is the molar flux of $ZrCl_4$ and $\vec{n}$, the normal to the surface.

4.3 BOUNDARY CONDITIONS

The surface reactions were treated as boundary conditions. The (Oz) velocity component v_z is assumed to be zero on the walls parallel to (Oz) and v_y on those parallel to (Oy). Azimuthal distribution of Ar-$ZrCl_4$ nuxture is assumed to be uniform. Furthermore, low substrate rotation ensures azimuthal deposition rate uniformity.
Species in the plasma are dissociated and recombine in the post-discharge to synthesize water. The partial pressure of water was determined by mass spectrometry measurements. The complete description of this measurement is given in[23]. The inlet flow rate of H_2O is taken equal to 15 sccm in the plasma conditions herein mentioned.
Temperatures are all measured, except for the inner and outer surfaces of the separating tube. The estimation of these temperatures has been achieved by considering that temperature of the quartz tube is equal to that of the furnace wall located at the same distance (same z as defined in figure 1). A complete calculation considering the quartz tube as a heat exchanger wall is available in[23] and show that this assumption is valid.

4.4 CALCULATION DATA

Transport properties are estimated by considering all the species as very diluted in argon. Kinetics constants of reactions (4) are taken from[23]. Each constant is given by an Arrhenius law :
$k_{s,v} = k^0_{s,v} \exp(-E_{s,v} / RT)$
For the surface reaction and the volume reaction, values are :
$k^0_s = 2.71 \times 10^{11}$ m^6 mol^{-2} s^{-1}, E_s =40 810 J mol^{-1}
$k^0_v = 1.32 \times 10^{13}$ m^6 mol^{-2} s^{-1}, E_v =88 570 J mol^{-1}
Computational mesh is cylindrical. It is 28x180 cells in r and z directions for 14 and 450 mm respectively. The funnel grid is approximated by 16x18 cells in r and z directions forming small steps.
Incorporating the axisymmetry assumption, the computational domain is reduced to a half of the reactor. The implicit Phoenics code is used for this calculation. Radial dimension is multiplied by a scale factor of 5 for the presentation of results (fig. 3 to 6).

5. RESULTS AND DISCUSSION

5.1 TEMPERATURES AND VELOCITIES DISTRIBUTION

At a furnace temperature of 753K, this temperature being that of the isothermal zone, temperatures distribution in the reactor is recorded in figure 3.

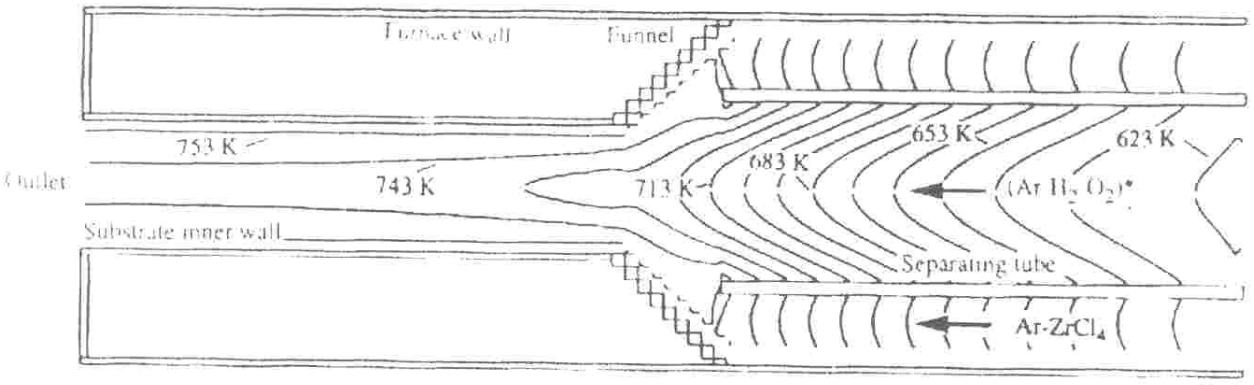

Figure 3 : Temperature distribution at a furnace temperature of 753K in conditions of table 1. Isolines are every 10 K.

The post-discharge mixture and the Ar-$ZrCl_4$ mixture are heated while flowing in the separating tube. The later reaches 753 K before entering the substrate whereas it is not the case of the former, its flow rate being too high. Therefore, the mixture of both gases in the funnel leads to the cooling of the Ar-$ZrCl_4$ mixture, and a radial temperature gradient of about 20 degrees occurs inside the substrate. This means that, over a distance of several centimeters, the gas phase reaction occurs at a lower temperature than that of the furnace wall.
Velocities of the gases are depicted in figure 4.

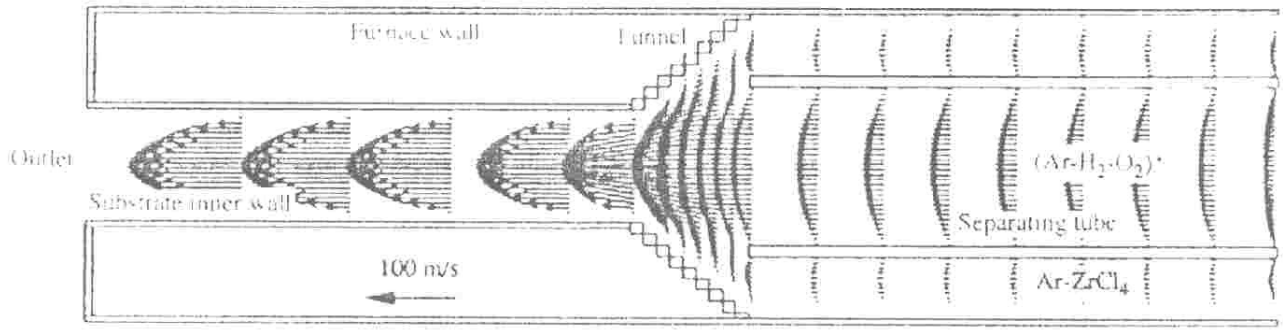

Figure 4 : Velocity distribution in the mixing-zone of Ar-$ZrCl_4$ with the post-discharge in conditions of table 1.

Flow is assumed to be laminar regardless of conditions (Re=150). The flow rate is high enough to avoid any recirculation in the mixing-zone of the post-discharge with gases flowing from the chlorination chamber. $ZrCl_4$ is essentially convected, in reference conditions, to the wall of the funnel. This can be observed by considering the mass fraction of $ZrCl_4$ (figure 5-b). In this figure, the mass fractions are given in a limited range because values outside this range variations are of little interest. Water mass fractions are given in figure 5-a. The role of the funnel that was expected to constrain gases inside the substrate is reached actually.

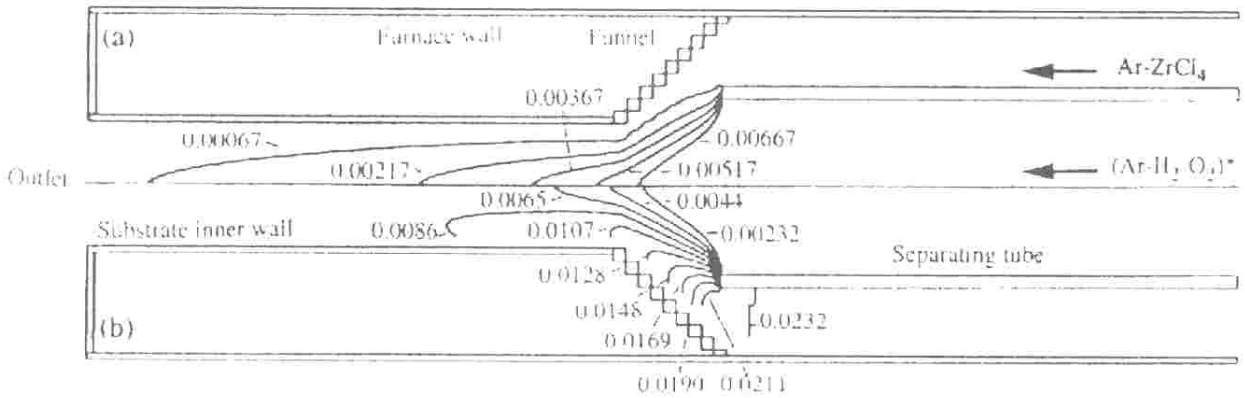

Figure 5 : $ZrCl_4$ and H_2O mass fraction distributions in the mixing-zone of Ar-$ZrCl_4$ with the post-discharge in reference conditions (isolines for H_2O are every 0.00067, only values in the range [0.00067-0.00667] are given, isolines for $ZrCl_4$ are every 0.00232, only values in the range [0.00232-0.0232] are given)

5.2 INFLUENCE OF MAIN PROCESS PARAMETERS ON DEPOSITION PROFILES

The experimental profiles of deposition rates at 673 K and 753 K (figures 6-b, 6-c) are nearly identical (figure 5). Both curves exhibit a maximum. The ascending part of the profiles is due to the mixing of Ar-$ZrCl_4$ with Ar-H_2O. The descending part is conversely due to reactive species consumption. On the funnel wall (figure 6-c), ZrO_2 deposition also occurs. Theoretical calculation including deposition on the funnel wall leads to the curve (c) in figure 6 but no experimental measurements were done to validate this result. A careful look at this curve permits to see a change of the slope at the transition between the cone and the plane before the substrate. In other cases, this part of the curve is no longer depicted.
One way to explain deposition rate remains unchanged while the temperature of the furnace decreases is by gas phase reaction. Deposition rate depends on temperature, but also on reactive species concentration. Therefore, effect of kinetic constant decrease (due to lower temperatures) can be explained by concentration increase (due to lower gas phase consumption) leading to constant deposition rate profiles[25]. The good agreement between

experimental results and calculated curves show that this description is probably valid.
For lower temperature (573 K), the deposition rate profile changes and the average rate increases (figure 6-a). Calculations and experimental results are no longer satisfying. This means that the increase of the average deposition rate can not be attributed to the correlated effects of surface and gas phase reactions.

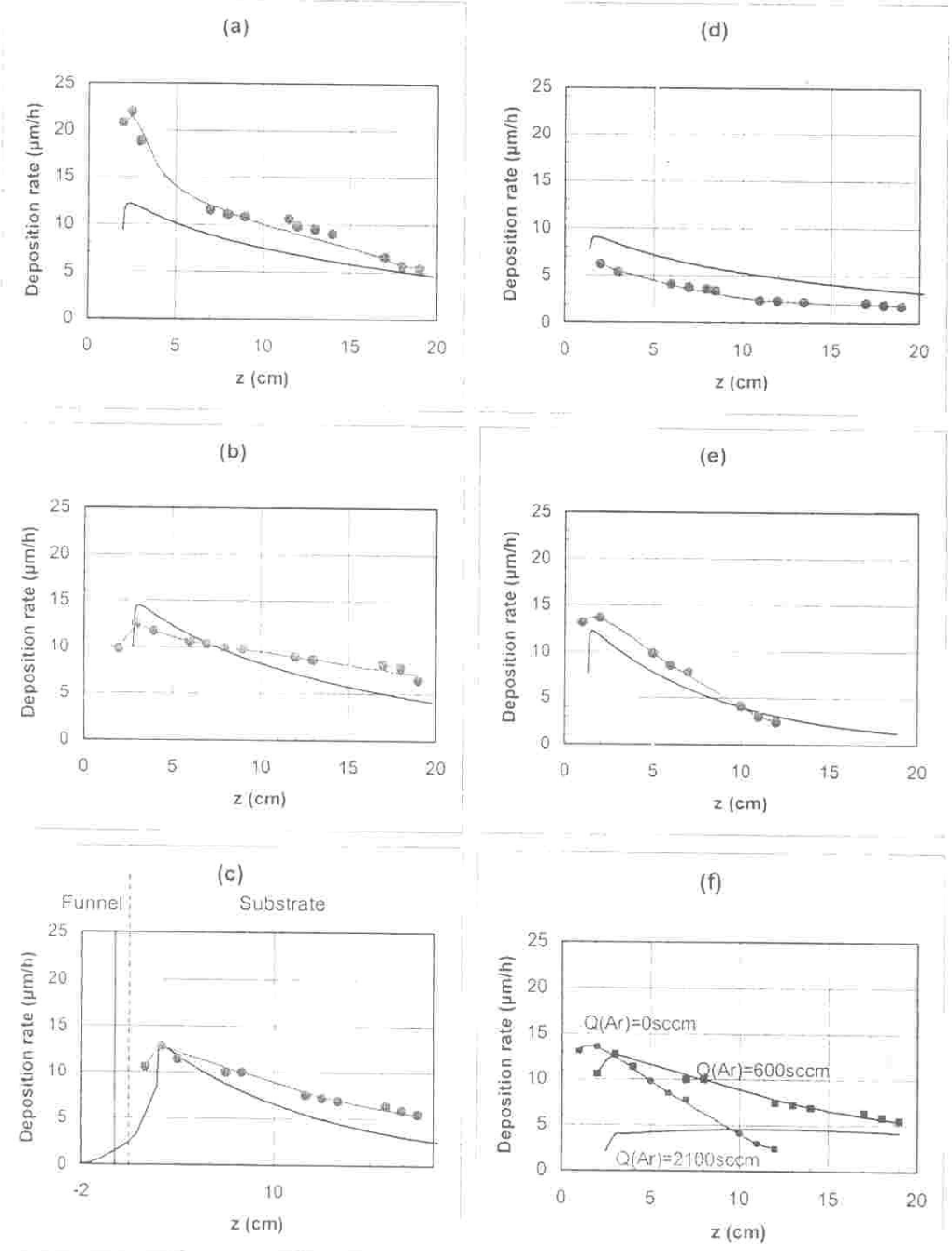

Figure 6 : Experimental (solid lines) and calculated (dotted lines) deposition rates versus location on the substrate in conditions of table 1 at (a) : 573 K, (b) : 673K, (c) : 753K, (d) Q($ZrCl_4$)=2sccm, T=753 K, (e) : Q(Ar in the additional line)=0sccm, T=753 K, (f) : Q(Ar in the additional line)=0, 600 and 2100 sccm, T=753 K. Deposition rate are given within the following error range : ± 5%.

An interesting hypothesis is the evolution that can be expected of the layer density. The shape of the layer's columns depends on the temperature and so the density. The difference observed between the calculation and the experimental result at 573 K is probably due to a decrease of the layer density. As explained above, the average diameter of a single crystal varies versus the temperature indeed. Furthermore, as the layer thickens, the divergence of the column induces an increase of the porosity. It is probably for this reason that the deposition rate strongly decreases in the first centimeters.

Influence of the flow rate of $ZrCl_4$ (figure 6-d) was determined. Dividing the chlorine flow rate by two leads to a decrease of the deposition rate by also a factor two, as this could be expected.

One way to obtain constant deposition rate over z is to increase the flow rate of argon carrying $ZrCl_4$, i.e. the argon flow rate in the additional line, which implies a dilution effect but also results in a better distribution over z of $ZrCl_4$. Nevertheless, $ZrCl_4$ convected to the funnel wall when argon flow rate is low, is available to react on the substrate, which offsets partially the dilution effect to give deposition rate still around 10µm/h. When the flow rate of argon carrying $ZrCl_4$ is increased from 0 (figure 6-e) to 600 sccm (figure 6-c), the deposition profile is flattened and the maximum position is slightly shifted.

Computer calculations show that deposition rate should be constant over 20 centimeters with a flow rate of argon in the additional line close to 2100 sccm (figure 6-f). In the experimental configurations studied, flat profiles could not be obtained with flow rates below 1400 sccm, i.e. the maximal flow rate available with the mass flow meters used here. New experiments will be carried out to check that almost constant deposition rate can be obtained in the conditions predicted by the model.

Temperature decrease leads also, in theory, to constant deposition rate, when surface reaction becomes rate limiting, but the structure of the layer is changed. Increasing the flow rate of argon in the Ar-$ZrCl_4$ mixture is also preferred to $ZrCl_4$ flow rate increase because calculations have demonstrated that very high chlorine flow rates should be used to reach constant deposition rate.

6. CONCLUSION

Treatment inside hollow substrates are possible by the CVD process herein described. Influence of the main parameters which do not affect plasma characteristics is described. A 2D hydrodynamic and chemical model of the chemical vapor deposition process is provided for given plasma parameters. This approach is very useful in its ability to describe a simple macroscopic deposition mechanism. Consumption of reactive species by gas phase reaction is taken into account. The gas distribution and deposition rate homogeneity over length are improved by increasing the velocity of argon in the Ar-$ZrCl_4$ mixture.

These findings should stimulate future work that will focus on plasma analysis to link plasma processes with transport phenomena and water synthesis. The future discussion of rate controlling steps involved in the process should also be considered.

BIBLIOGRAPHY

1 E.T. Kim and S.G. Yoon, Thin Solid Films 227 (1991) 7

2 G. Seiberras, C. Indrigo, V. Rousseau, P. Leprince and R. Mevrel, Conférence Internationale sur les Plasmas Antibes (1993) 375

3 X. Illus, M. Viennot, D. David, D. Hertz and H. Michel, J. of Nuclear Mat. 209 (1994) 80

4 J. Gavillet, T. Belmonte, D. Hertz, H. Michel, Thin Solid Films 301 (1997) 35.

5 K. Brennfleck, E. Fitzer, G. Mack, in J.M. Blocher, G.E. Vuillard and G. Wahl (eds.), Proc. CVD VIII, Eindhoven (1983) 44

6 M.H.J.M. De Croon, L.J. Giling, J. Electrochem. Soc. 137 9 (1990) 2867

7 A. Kwatera, Ceramics International 17 (1991) 11

8 S. Rhee, J. Szekely, O.J. Ilegbusi, J. Electrochem. Soc. 134 10 (1987) 2552

9 M.J. Hartig, M.J. Kushner, J. Appl. Phys. 62 14 (1993) 1594

10 S.K. Dew, T. Smy, M.J. Brett, J. Vac. Sci. Technol. B 10 2 (1992) 618

11 W.G. Houf, J.F. Grear, W.G. Breiland, Materials Science and Engineering B 17 (1993) 163

12 K.W. Schröder, J. Schlote, S. Hinrich, J. Electrochem. Soc. 138 8 (1991) 2466

13 E. Whitby, K. Tsuzuki, IEICE Trans. Electron. E75-C 7 (1992) 852

14 C. Weber, C. van Opdorp, M. de Keijser, J. Appl. Phys. 67 4 (1990) 2109

15 G. Evans, R. Greif, Trans. of the ASME : J. of Heat Transfer 109 (1987) 928

16 D.I. Fiotadis, M. Boekholt, K.F. Jensen, W. Richter, J. of Crystal Growth 100 (1990) 577

17 E.P. Visser, C.R. Kleijn, C.A.M. Govers, C.J. Hoogendoorn, L.J. Giling, J. of Crystal Growth 94 (1989) 929

18 K.F. Roenig, K.F. Jensen, J. Electrochem. Soc. : Solid State Science 134 7 (1987) 1777

19 P.W. Brown, D. Zhu, Y. Sahai, First International Conference on Transport Phenomena in processing. Ed. by Selcuk I Guceri, Honolulu, Hawaii (1992) 113

20 K.L. Knutcn, R.W. Carr, W.H. Liu, S.A. Campbell, J. of Crystal Growth 140 (1994) 191

21 C. Theodoropoulos, N.K. Ingle, T.J. Moutziaris, Z-Y. Chen, P.L. Liu, G. Kioseoglu, A. Petrou, J. Electrochem. Soc. 142 6 (1995) 2086

22 M. de Keijser, G.J.M. Dormans, J. of Crystal Growth 149 (1995) 215

23 T. Belmonte, J. Gavillet, T.Czerwiec, H. Michel, J. Phys. III France, 7 (1997) 1779

24 S. Meikle, H. Nomura, Y. Nakanishi and Y. Hatanaka, J. Appl. Phys. 67 1 (1990) 483

25 K.J. Sladek, J. Electrochem. Soc.: Solid State Science 118 4 (1971) 654